Pulmonary hypertension due to left heart disease causes intrapulmonary venous arterialization in rats

CrossMark

Yoshitaka Fujimoto, MD,[a,b] Takashi Urashima, MD, PhD,[b] Fumie Kawachi, MD,[a,b] Toru Akaike, MD, PhD,[a] Yoichiro Kusakari, MD, PhD,[a] Hiroyuki Ida, MD, PhD,[b] and Susumu Minamisawa, MD, PhD[a]

CONG

ABSTRACT

Objective: A rat model of left atrial stenosis–associated pulmonary hypertension due to left heart diseases was prepared to elucidate its mechanism.

Methods: Five-week-old Sprague–Dawley rats were randomly divided into 2 groups: left atrial stenosis and sham-operated control. Echocardiography was performed 2, 4, 6, and 10 weeks after surgery, and cardiac catheterization and organ excision were subsequently performed at 10 weeks after surgery.

Results: Left ventricular inflow velocity, measured by echocardiography, significantly increased in the left atrial stenosis group compared with that in the sham-operated control group (2.2 m/s, interquartile range [IQR], 1.9-2.2 and 1.1 m/s, IQR, 1.1-1.2, $P < .01$), and the right ventricular pressure-to-left ventricular systolic pressure ratio significantly increased in the left atrial stenosis group compared with the sham-operated control group (0.52, IQR, 0.54-0.60 and 0.22, IQR, 0.15-0.27, $P < .01$). The right ventricular weight divided by body weight was significantly greater in the left atrial stenosis group than in the sham-operated control group (0.54 mg/g, IQR, 0.50-0.59 and 0.39 mg/g, IQR, 0.38-0.43, $P < .01$). Histologic examination revealed medial hypertrophy of the pulmonary vein was thickened by 1.6 times in the left atrial stenosis group compared with the sham-operated control group. DNA microarray analysis and real-time polymerase chain reaction revealed that transforming growth factor-β mRNA was significantly elevated in the left atrial stenosis group. The protein levels of transforming growth factor-β and endothelin-1 were increased in the lung of the left atrial stenosis group by Western blot analyses.

Conclusions: We successfully established a novel, feasible rat model of pulmonary hypertension due to left heart diseases by generating left atrial stenosis. Although pulmonary hypertension was moderate, the pulmonary hypertension due to left heart diseases model rats demonstrated characteristic intrapulmonary venous arterialization and should be used to further investigate the mechanism of pulmonary hypertension due to left heart diseases. (J Thorac Cardiovasc Surg 2017;154:1742-53)
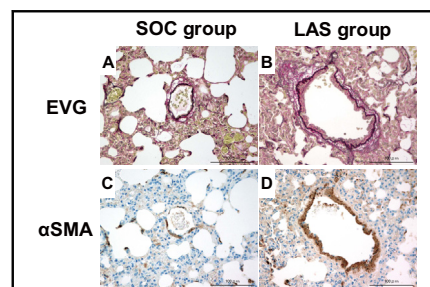
The medial wall of the PV was thickened in the LAS group.

Central Message

We prepared a PH-LHD rat model based on hemodynamics by increasing the left atrial and pulmonary venous pressure.

Perspective

PH-LHD is the most frequent cause of PH. Although PAH has been intensively investigated, PH-LHD remains unclear because of the lack of an appropriate PH-LHD animal model. In this study, we generated a novel PH-LHD rat model. TGF-β and endothelin-1 were significantly increased in this model. Further investigation will reveal a new mechanism and treatment for PH-LHD.

See Editorial Commentary page 1754.

Pulmonary hypertension (PH) due to left heart disease (LHD) is the most common form of PH. PH-LHD belongs to the second group in the World Health Organization classification that was updated in Nice.[1,2] Primary LHD consists of heart failure (HF) with reduced or preserved ejection fraction and severe left-sided valvular diseases, such as mitral valve stenosis. It has been recently reported that the presence of PH-LHD in patients with left

---

Abbreviations and Acronyms

ET	=	endothelin
HF	=	heart failure
HR	=	heart rate
IQR	=	interquartile range
LA	=	left atrium
LAS	=	left atrial stenosis
LHD	=	left heart disease
PA	=	pulmonary artery
PAH	=	pulmonary arterial hypertension
PCNA	=	proliferating cell nuclear antigen
PDE	=	phosphodiesterase
PDE-5	=	phospodiesterase-5
PH	=	pulmonary hypertension
PV	=	pulmonary vein
PVS	=	pulmonary vein stenosis
RV	=	right ventricular
SMA	=	smooth muscle actin
SOC	=	sham-operated control
TGF	=	transforming growth factor
VEGF	=	vascular endothelial growth factor

📎 Scanning this QR code will take you to supplemental figures, tables, and videos for this article.

HF is associated with a worse prognosis than in those without PH-LHD.[3] Despite its prevalence and significance, there has been little research on PH-LHD. Moreover, no effective drug regimen has been established, and treatment is usually for the underlying LHD. For example, phospodiesterase-5 (PDE-5) inhibitors are clinically used for patients with PH-LHD[4-6]; however, the efficacy of PDE-5 inhibitors against PH-LHD is controversial[7] because the use of pulmonary vasodilators elevates left atrial pressure in those with PH-LHD, which may worsen congestive HF.

In addition, the pathophysiology of PH in PH-LHD should be different from that of pulmonary arterial hypertension (PAH), in which there is remodeling of the pulmonary artery (PA).[8] A main cause of the lack of clarity surrounding the treatment and mechanism in PH-LHD could be the absence of an appropriate PH-LHD animal model. The objective of this study is to establish a PH-LHD rat model based on the hemodynamic mechanism accompanying left atrial stenosis (LAS)-induced left atrial pressure elevation and observe changes in the lung to elucidate the mechanism of PH-LHD.

MATERIALS AND METHODS

Experimental Design

Five-week-old Sprague-Dawley rats were purchased from the same trader (Sankyo Labo Service Corporation, Tokyo, Japan) and installation date, and randomly divided into LAS and sham-operated control (SOC) groups. For example, we purchased 2 rats for a 1-day surgical procedure and then divided them into 1 for LAS and 1 for SOC. The protocol of this study is shown in Figure 1. Animals were intubated with Angiocath 18G under 2% isoflurane anesthesia, and respiration was managed using a Harvard rodent ventilator (Harvard Apparatus, Holliston, Mass), in which the tidal volume was set at 10 μL/g, and the respiratory rate was set at 100/min in accordance with a previous study.[9] The thymus was removed by lateral thoracotomy through the fifth intercostal region. Because the thymus was stuck with the epicardium, we needed to remove the thymus. The heart was identified, and an interrupted suture was applied to the left atrial appendage using 5-0 Prolene (Johnson and Johnson, New Brunswick, NJ) in the LAS group (n = 5). The thread of the interrupted suture was pulled up to lift the heart, and the left atrium (LA) was half clipped under direct vision using Horizon Ligating Clips (Teleflex, Morrisville, NC) and a Horizon Manual-Load ligating Clip Applier (Teleflex). The thorax was then closed. The procedure is shown in Videos 1 and 2. When left ventricular (LV) inflow velocity was 2.0 m/s or higher on echocardiography at 2 weeks after surgery, the rats were subjected to further analysis. Because LV inflow velocity of 2.0 m/s or higher is considered significant in human mitral valve stenosis,[10] we used the LV inflow velocity of 2.0 m/s for a cutoff value to estimate the PH-LHD model rats. In the SOC group (n = 5), only thymectomy was performed and the thorax was then closed. We set the observation period for 10 weeks after surgery, because Wang and colleagues[11] previously reported that aortic constriction caused PH-LHD 9 weeks after surgery. All rats were maintained at $22°C ± 2°C$ under a 12-hour light/dark cycle following the National Institute of Health guidelines for animal experiments. This experiment was performed after approval by the Institutional Animal Care and Use Committee of The Jikei University (2015-118C1).

Echocardiography

Echocardiography was performed at 2, 4, 6, and 10 weeks after surgery in both groups, and the rats were sedated with 1.5% isoflurane using a

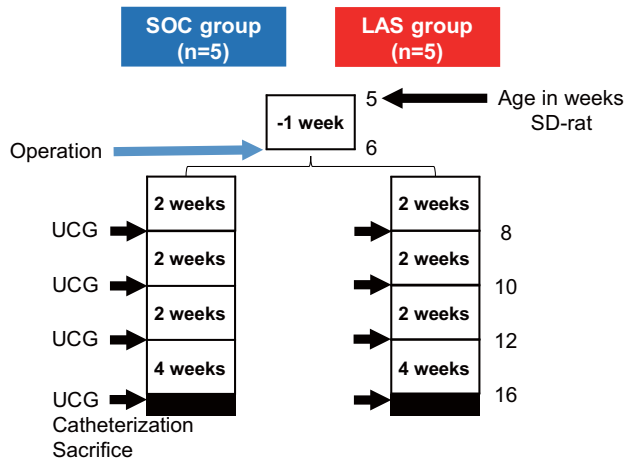**FIGURE 1.** Study protocol of the SOC and LAS groups. Five-week-old Sprague–Dawley rats were randomly divided into the LAS and SOC groups. Ultrasound cardiography was performed 2, 4, 6, and 10 weeks after surgery, and cardiac catheterization and organ excision were performed 10 weeks after surgery. *SOC,* Sham-operated control; *LAS,* left atrium stenosis; *SD,* Sprague–Dawley; *UCG,* ultrasound cardiography.

VIDEO 1. Surgical method. The thread of the interrupted suture was pulled up to lift the heart, and the LA was half clipped under direct vision using Horizon Ligating Clips and Horizon Manual-Load ligating Clip Applier (Teleflex, Morrisville, NC). Video available at: http://www.jtcvsonline.org/article/S0022-5223(17)31372-7/addons.

13-MHz transducer from the GE Vivid i8 ultrasound system (GE Healthcare, Madison, Wis). The parameters of echocardiography were also used in a previous study.[9]

Cardiac Catheterization

Cardiac catheterization was performed at 10 weeks after surgery under 2% isoflurane anesthesia using artificial respiration management. The artificial respiration conditions were the same as those during surgery. We used 1.9F Rodent PV Catheters (Transonic Systems Inc, Ithaca, NY) and the ADVantage PV System (Transonic Systems Inc) for measuring pressure and volume of right ventricles (RVs) and LV, and then analyzed the data using the analysis software Labscribe2 (iWorx, Dover, NH). RV and LV pressures were measured by directly placing the catheter into each ventricle after thoracotomy. After completion of catheterization, the animals were euthanized with pentobarbital and the organs were excised. Estimated LA pressure was calculated by adding LV end-diastolic pressure and the pressure gradient between LV and LA. The pressure gradient between LV and LA was measured by echocardiography using Bernoulli's principle from the blood flow velocity in the clip region. LV end-diastolic pressure was measured by cardiac catheterization.

Histologic Examination and Measurement of Venous Wall Thickness

The excised lung tissue was subjected to hematoxylin–eosin, Masson-trichrome, and Elastica van Gieson staining. Each sample was observed under a light microscope at 40 times magnification, and 8 (100-300 μm) pulmonary veins (PVs) were randomly selected per sample and photographed. In the photographed images, the venous and venous luminal areas were measured using Image-Pro Premier 9.1 (Media Cybernetics, Rockville, Md) (Figure E1). This method also was used by

VIDEO 2. Degree of half clip. The degree of half clip was modulated to make the 2 front edges attached to each other. Video available at: http://www.jtcvsonline.org/article/S0022-5223(17)31372-7/addons.

Nishimura and colleagues,[12] who calculated the venous wall thickness by subtracting the venous lumen from the venous area.

Immunostaining of Lung Tissue

Immunostaining of α-smooth muscle actin (SMA) (mouse anti-human antibody, M0851, DakoCytomation, Glostrup, Denmark), proliferating cell nuclear antigen (PCNA) (mouse anti-human antibody, M0879, DakoCytomation), Ephrin B2 (rabbit anti-mouse antibody, NBP1-84830, Novus Biologicals, Littleton, Colo), and EphB4 (goat anti-human antibody, sc7285, Santa Cruz Biotechnology, Dallas, Tex) was performed in 5 rats each in the LAS and SOC groups.

DNA Microarray Analysis

For Oligo DNA microarray analysis, 3D-Gene Rat Oligo chip 20k (Toray Industries Inc, Tokyo, Japan) was used. Two lung samples from each group were combined for comparison. Total RNA was labeled with Cy5 using the Amino Allyl MessageAMP II aRNA Amplification Kit (Applied Biosystems, Foster City, Calif). The Cy5-labeled aRNA pools and hybridization buffer were hybridized for 16 hours. The hybridization was performed using the supplier's protocols (www.3d-gene.com). Hybridization signals were scanned using ScanArray Express Scanner (PerkinElmer, Waltham, Mass) and processed by GenePixPro version5.0 (Molecular Devices Inc, Sunnyvale, Calif). The raw data intensities greater than 2 standard deviations of the background signal intensity were considered to be valid. Detected signals for each gene were normalized using a standard normalization method.

Real-Time Polymerase Chain Reaction Analysis

Both isolation of total RNA from pooled tissues and generation of cDNA and reverse transcription-polymerase chain reaction analysis were performed as described previously.[9] Transforming growth factor-β1 (TGF-β1), αSMA, vascular endothelial growth factor (VEGF), endothelin-1 (ET-1), endothelin type A receptor, endothelin type B receptor, procollagen I, and connective tissue growth factor expression levels in the lung were measured in the LAS (n = 5) and SOC (n = 5) groups using real-time polymerase chain reaction. The primer nucleotide
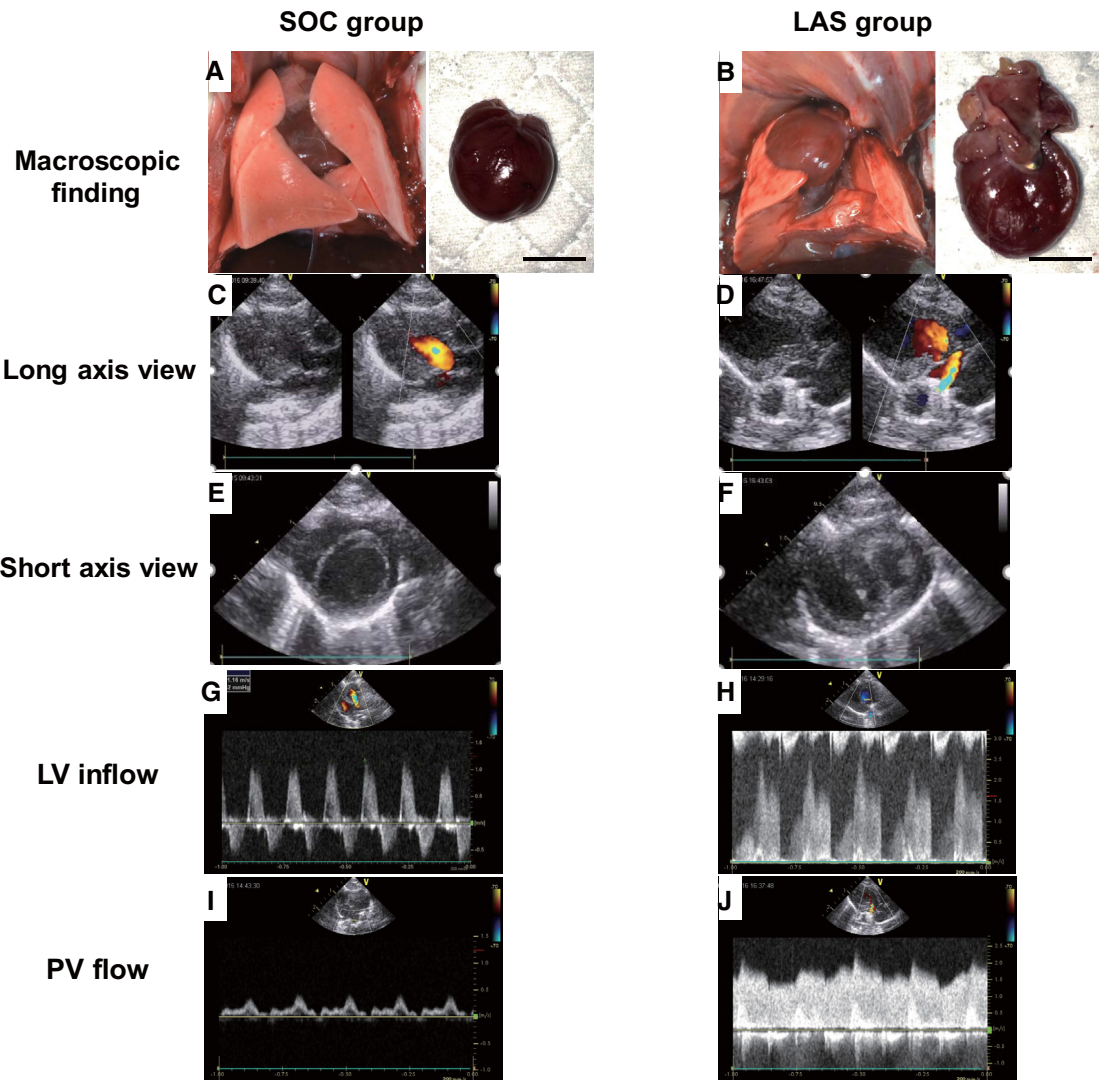
SOC group

LAS group

FIGURE 2. Macroscopic and echocardiographic findings in the SOC and LAS groups. A, Macroscopic finding of the SOC group. B, Macroscopic finding of the LAS group shows LA dilatation, pulmonary effusion and congestion. Long-axis (C) and short-axis (E) views of the SOC group. Long-axis (D) and short-axis (F) views of LAS group. In short-axis view, the interventricular septum flattened with an increase in wall thickness in the LAS group. G, LV inflow of the SOC group. H, LV inflow velocity was accelerated from the clipped region in the LAS group. I, PV flow of the SOC group. J, PV flow of the LAS group showed continuous waves. *SOC*, Sham-operated control; *LAS*, left atrium stenosis; *LV*, left ventricle; *PV*, pulmonary venous. Bar of A and B: 10 mm of the SOC group (F).

sequences are shown in Table E1. The 18S RNA expression level was quantitated as an internal reference.

Western Blot Analysis

Total protein was extracted from the lung and used for Western blot analyses including antibodies against ET-1 (mouse anti-human antibody, ab2786, Abcam, Cambridge, UK), TGF-β (rabbit anti-human antibody, #3711, Cell Signaling, Danvers, Mass), and β-actin (mouse anti-human antibody, 122M4782, Sigma-Aldrich, St Louis, Mo), as described previously.[9]

Statistical Analysis

Statistical analyses were performed using Prism 7 (GraphPad Software, Inc, La Jolla, Calif). All data are presented as the mean ± standard deviation or interquartile range. Two-way repeated-measures analysis of variance followed by Sidak's post hoc test was performed to assess

echocardiographic finding. Other analyses were performed using the Mann–Whitney U test.

RESULTS

The Left Atrial Stenosis Group Developed Pulmonary Hypertension and Left Heart Disease

Rats that underwent LAS developed a dilated LA, marked congestion, and pleural effusion 10 weeks after surgery (Figure 2, *A* and *B*). We confirmed at autopsy that the circumflex coronary artery was not clipped in the LAS group. The summary of heart weight measurement and hemodynamic parameters is shown in Table 1. The ratio of RV to body weights was significantly increased by approximately 1.5 times in the LAS group compared with

TABLE 1. Operative and cardiac catheterization parameters, and estimated left atrial pressure in the sham-operated control and left atrial stenosis groups

Operative parameters	SOC group (n = 5)		LAS group (n = 5)		P value
	Median	IQR	Median	IQR	
BW operation (g)	195	190-205	194	190-208	.98
BW sacrifice (g)	416	410-420	452	390-505	.65
RV weight/BW	0.39	0.38-0.43	0.54	0.50-0.59	<.01
LV weight/BW	1.91	1.85-1.95	1.98	1.78-2.2	.69
RV weight/LV weight	0.2	0.19-0.22	0.27	0.27-0.28	<.01
Lung weight/BW	0.37	0.36-0.41	0.47	0.42-0.51	<.01
Cardiac catheterization					
RV systolic pressure (mm Hg)	18	16-20	40.6	30-50	<.01
RV end-diastolic pressure (mm Hg)	1.6	1.0-2.0	3.4	3.0-4.0	<.01
LV systolic pressure (mm Hg)	84	60-80	77.6	70-80	.72
LV end-diastolic pressure (mm Hg)	2.8	2.0-3.0	7.6	7.0-8.0	.013
RV systolic pressure/LV systolic pressure	0.22	0.15-0.27	0.52	0.54-0.60	.021
Estimated LA pressure (mm Hg)	7.9	6.8-8.4	28.1	22.8-27.0	<.01

SOC, Sham-operated control; LAS, left atrium stenosis; IQR, interquartile range; BW, body weight; RV, right ventricle; LV, left ventricle; LA, left atrium.

that in the SOC group (Table 1). The ratio of lung to body weights was significantly increased in the LAS groups.

The RV pressure was significantly increased in the LAS group, as the representative pressure waveforms are shown in Figure E2. Although we could not directly measure PA pressure, the RV systolic pressure/LV systolic pressure ratio in the LAS group was significantly increased to 0.52 (interquartile range, 0.54-0.60), indicating moderate PH (Table 1). In addition, the end-diastolic LV and RV pressures were significantly
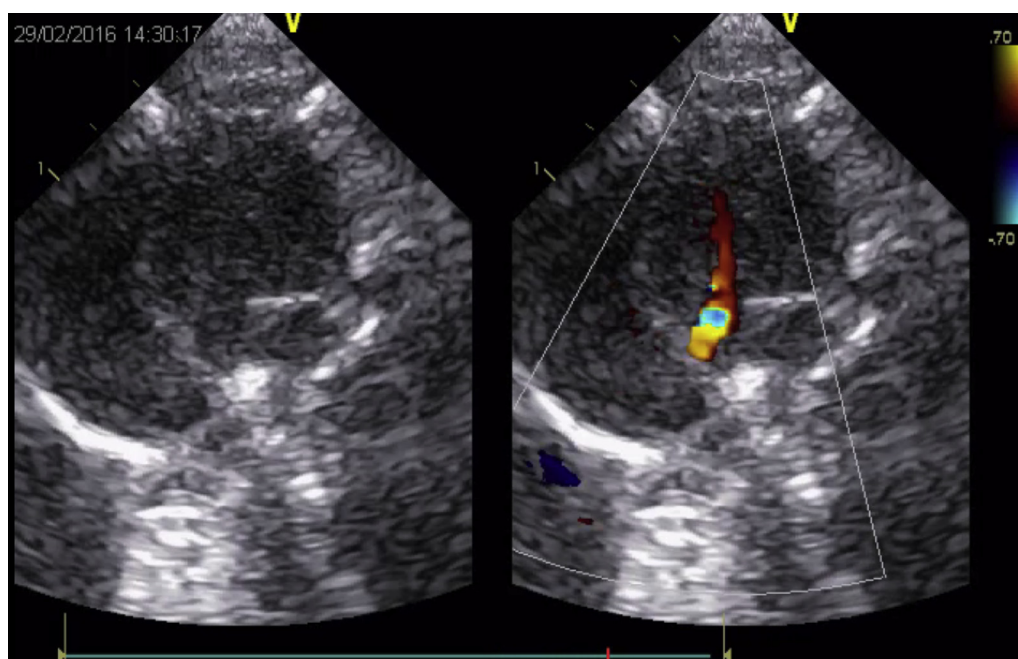
VIDEO 3. Four-chamber view of the LAS group by echocardiography. An artifact produced by clipping was noted in the LA in the LAS group. Video available at: http://www.jtcvsonline.org/article/S0022-5223(17)31372-7/addons.
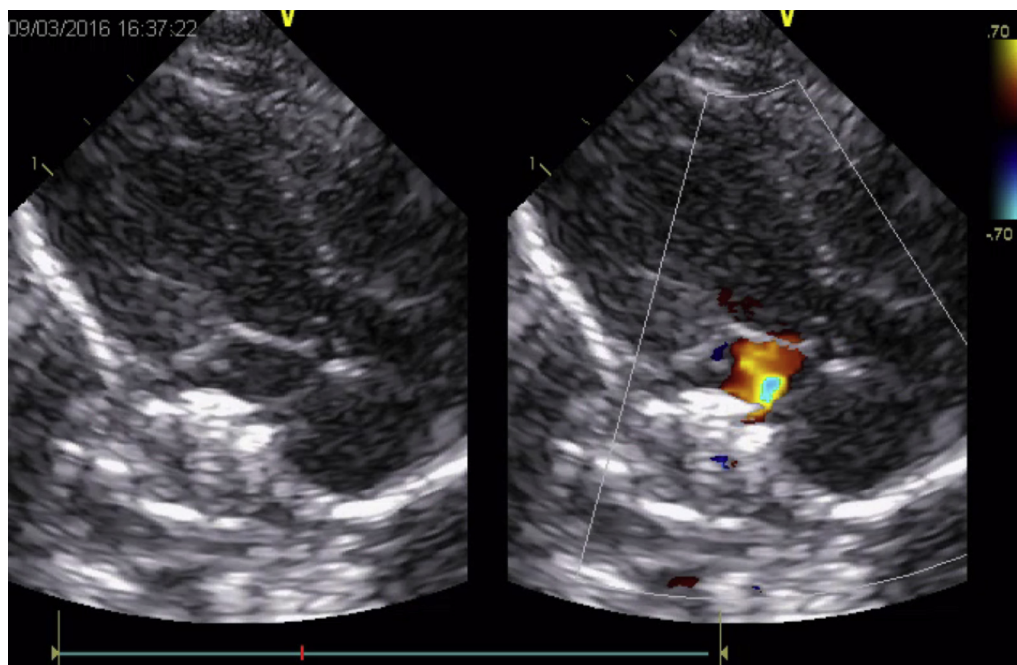
VIDEO 4. Long-axis view of LAS group by echocardiography. LV inflow velocity is accelerated from the clipped region in color Doppler images. Video available at: http://www.jtcvsonline.org/article/S0022-5223(17)31372-7/addons.

higher in the LAS group compared with the SOC group (Table 1).

Representative images of echocardiography at 10 weeks after surgery are shown in Figure 2 and Videos 3 and 4. In the long-axis and 4-chamber views, an artifact produced by clipping was noted in the LA in the LAS group. Color Doppler imaging revealed that LV inflow velocity was accelerated from the clipped region. In the short-axis view, the interventricular septum flattened with an increase in wall thickness, suggesting that RV pressure was increased. Pulmonary venous blood flow showed continuous waves of 2 animals in the LAS group.

Changes in the echocardiographic findings after surgery are shown in Figure 3. The LV inflow velocity was approximately 2 times higher in the LAS group than in the SOC group. Left ventricular ejection fraction was gradually decreased in the LAS group, but it was not significant. Cardiac output was significantly decreased in the LAS group. LA dimensions were enlarged at 6 and 10 weeks after surgery in the LAS group compared with the SOC group.

The Medial Wall of the Pulmonary Vein Was Thickened in the Left Atrial Stenosis Group

We found pulmonary arteriovenous congestion and venous dilatation in the LAS group (Figures 4 and E3). On Elastica van Gieson staining, the isolated medial hypertrophy of muscular pulmonary arteries with an outer diameter of 100 to 300 μm was observed in the 4 rats of LAS group, but that no neointimal lesion developed (Figure 4, C).

In addition, the venous wall thickness and dimension were significantly increased in the PVs with an outer diameter of 100 to 150 μm in the LAS group (Figure 4, V and W). αSMA staining was positive in these pulmonary venous walls, and the smooth muscle thickness was increased in the LAS group compared with the SOC group (Figure 4, F and H). PCNA immunostaining identified PCNA-positive cells more in the PV smooth muscle of the LAS group than in the SOC group, suggesting an increase in proliferative ability in the LAS group (Figure 4, X) (15.55 $\pm$ 5.18 and 7.51 $\pm$ 3.98, respectively, $P < .01$). Ephrin B2 was expressed in the endothelial cells of the PA and vein of each group, but no EphB4 expression was observed in both groups (Figure 4, M-T).

Transforming Growth Factor-β and Endothelin Signal Pathways Could Be Enhanced in the Left Atrial Stenosis Group

DNA microarray analysis identified the genes with expression levels were 4 times or greater different between the LAS and the SOC groups (Figure 5 and Table E2). Pathway analysis identified that the TGF-β signaling pathway was an enhanced pathways in the LAS group (Figure E4). The TGF-β signaling pathway is known as a therapeutic target in patients with PH. In addition, the pathway promotes the tissue fibrosis. Thus, we evaluated mRNA expression of TGF-β1, connective tissue growth factor, procollagen I (barometer of fibrosis), αSMA (activated by TGFβ1), VEGF (factor of angiogenesis),
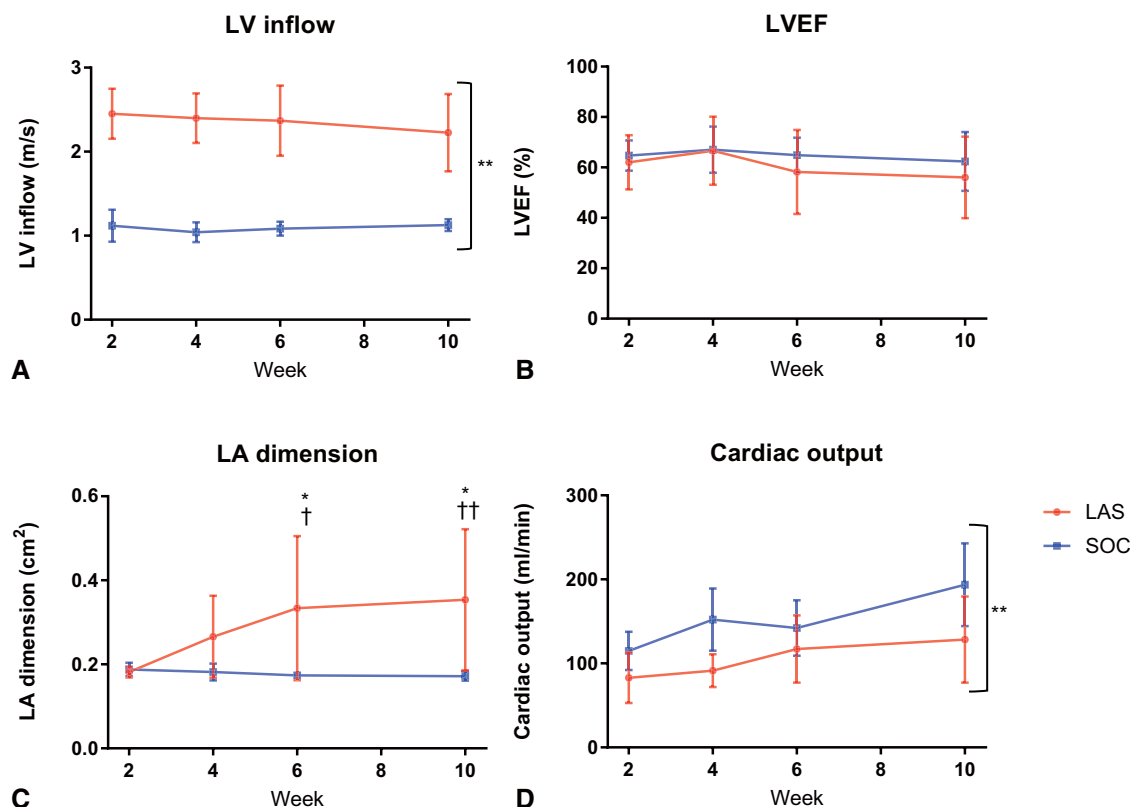
CONG

CONG

FIGURE 3. Echocardiographic parameters of the SOC and LAS groups. A, LV inflow velocity was approximately 2 times higher in the LAS group (n = 5) than in the SOC group (n = 5). B, Left ventricular ejection fraction was gradually decreased in the LAS group. C, LA dimensions were significantly enlarged at 10 weeks after surgery in the LAS group. D, Cardiac output significantly decreased in the LAS group compared with the SOC group at 10 weeks after surgery. *LV,* Left ventricle; *LVEF,* left ventricular ejection fraction; *LA,* left atrium; *LAS,* left atrium stenosis; *SOC,* sham-operated control. *P < .05 SOC versus LAS at the same time point. **P < .01 SOC versus LAS. †P < .05. ††P < .01 LAS at 6 and 10 weeks after surgery versus LAS at 2 weeks after surgery.

ET-1 (regulated by TGFβ1), and endothelin type A and endothelin type B receptor (receptors for ET-1).

On real-time polymerase chain reaction, the αSMA and VEGF expression levels were higher in the LAS than in the SOC group (LAS: 6.98 ± 1.37 and 2.87 ± 0.67, respectively, $P < .01$; SOC: 1.0 ± 0.40 and 1.0 ± 0.21, respectively, $P < .01$). TGF-β1, ET-1, endothelin type A, endothelin type B, connective tissue growth factor, and pro-collagen I mRNA expression were not different between 2 groups (Figure 6, *A-H*). Western blot analyses revealed that TGF-β1 and ET-1 protein expression were significantly increased in the LAS group compared with the SOC group (Figure 6, *I-K*).

DISCUSSION
Left Atrial Stenosis–Induced Pulmonary Hypertension Left Heart Disease Model Is a Unique Pulmonary Hypertension Model

The most important finding in the present study is that progressive medial hypertrophy was observed in the PVs of a PH-LHD rat model, which resulted from PV congestion that prevented PV flow by clipping the LA lesion. In this PH-LHD rat model, moderate medial hypertrophy also

was observed in the PA. To the best of our knowledge, this is the first animal model of PH-LHD induced by LAS.

The pathophysiology of PH-LHD is different from the other kinds of PH.[13] Thus, appropriate animal models are required to elucidate its mechanism for the detailed research. There are 2 PH-LHD models reported: the pulmonary vein stenosis (PVS) model using piglets and the aortic banding rat model.

Kato and colleagues[14] applied banding to the PVs in an in vivo experiment using a PVS model in piglets, in which an increase in the wall thickness of the upstream PV in the lung was also observed in this model, which is similar to the observations in our study. In a LAS-induced PH-LDH model, we also found that medial hypertrophy was more marked in smaller PVs and those further away from the LAS lesion (Figure 4, *U*). This indicates that the influence of LAS gradually expands upstream in the lung. αSMA and TGF-β were also upregulated in the PVs in both studies. Therefore, our rat model phenotype of LAS-induced PH-LDH closely resembles that of the piglet model of PVS, although PH induction was not clearly demonstrated in the PVS model. However, our rat model of LAS-induced PH-LDH has some advantages over a piglet PVS
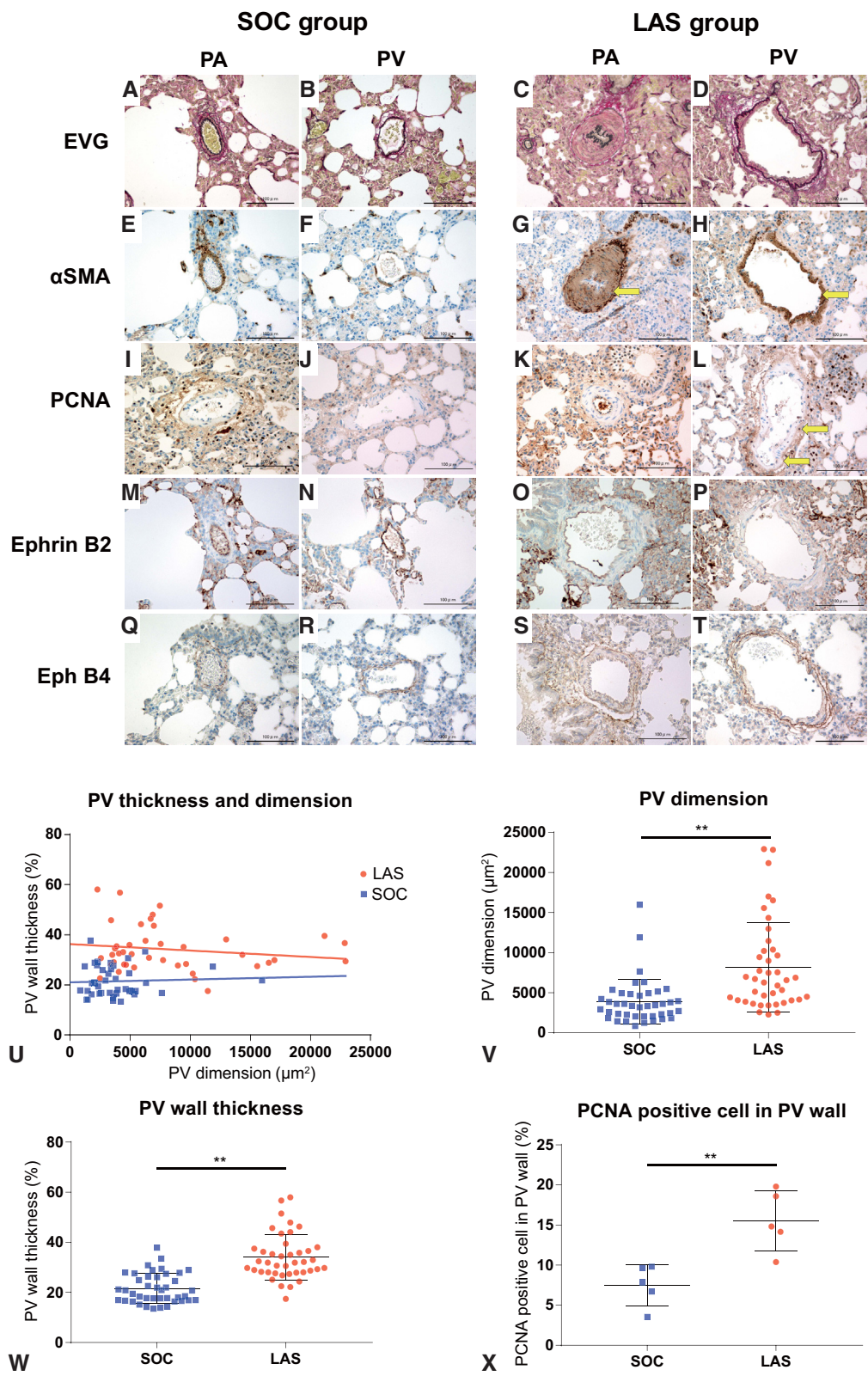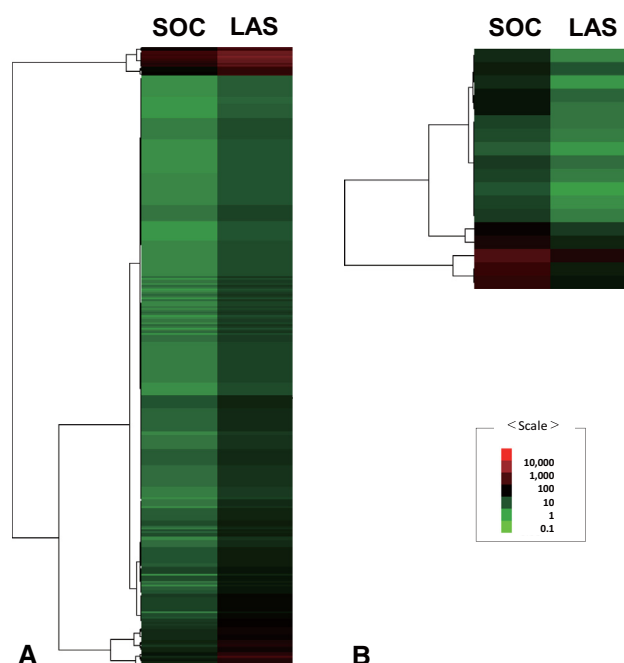
FIGURE 5. Heat map in the SOC and LAS groups. DNA microarray analysis using 3D-Gene Rat Oligo chip 20k identified the genes with expression levels were (A) 4 times or greater and (B) one quarter times or less different between the LAS and the SOC groups. *SOC,* Sham-operated control; *LAS,* left atrium stenosis.

model: The surgical procedure to generate LAS is easier and less complicated than that of PVS, and the rat is a widely used experimental animal with a lower cost.

Aortic banding was also used to prepare a PH-LHD rat model in some previous studies.[11,15,16] These models demonstrated mild PH and left HF. Wang and colleagues[11] reported that pulmonary arterial medial thickening and biventricular cardiac hypertrophy are observed, and PCNA-positive cells are noted in vascular SMCs in their aortic banding models. These results are also observed in our study. However, this method is not ideal because it has several disadvantages. PH caused by aortic stenosis is relatively rare in humans. PH-LDH caused by mitral valve lesions is more common, and its hemodynamics are similar to those of our LAS model.[17]

In addition, the aortic banding model also initially promotes left HF, and pulmonary congestion occurs thereafter. Therefore, the pathophysiology of PH-LHD by aortic banding is complicated compared with LAS-induced PH-LHD.

Animal models of PAH such as monocrotaline-treated rats, hypoxic rats, and Sugen5416 VEGF antagonist–treated rats have been established. Moreover, 2-hit models combining 2 elements (eg, hypoxia and Sugen5416) have been developed as a model of PAH. In these rats, pathologic findings are similar to those of PAH in humans (ie, PAH begins with medial hypertrophy of small pulmonary arteries, and plexiform lesions then appear after neointimal lesions).[18-23] However, except for hypoxia, the effects of monocrotaline and Sugen5416 are artificial and different from the cause of PAH in humans. These studies focused on pulmonary arterial changes, not on the PV. Developing pulmonary congestion and pulmonary edema is the most critical difference between PH-LHD and PAH. Although we did not measure hydrostatic pressure of the PV, it should be high in a PH-LHD model based on its hemodynamics and the findings of pleural effusion. Pulmonary congestion could increase the alveolar-arterial oxygen difference, which is not usually observed in a PAH model. Although these differences should affect PH progression, there are few insights into how the mechanism and development of PH in PH-LHD and PAH are different. Therefore, LAS in the present study should be a reasonable and feasible method to investigate the mechanisms of PH-LHD.

Pulmonary Vein Remodeling in Pulmonary Hypertension Left Heart Disease

Endo and colleagues[24] demonstrated that central PV obstruction is known to trigger pulmonary venous arterialization, progressive medial hypertrophy, and intimal fibrosis of the affected venous tree. Because we found that medial hypertrophy was developed and αSMA and PCNA were positive in the wall of the PV in the LAS group, we think that the veins are arterialized. Although the mechanism of pulmonary venous arterialization still remains unclear. It has been reported that arterialization of

FIGURE 4. Pathologic changes in the lung of LAS groups. The PA (A, C) and PV (B, D) of the SOC and LAS groups stained by Elastica van Gieson, respectively. The medial wall of PA was thickened, and venous wall thickness and dimension were significantly increased in the LAS group. PA (E, G) and PV (F, H) of the SOC and LAS groups stained by αSMA immunostaining, respectively. The positive cells were observed in vessel walls of the LAS group (*yellow arrow*). PA (I, K) and PV (J, L) of the SOC and LAS groups stained by PCNA immunostaining, respectively. PCNA-positive cells were found in the PV of the LAS group (*yellow arrow*). PA (M, O) and PV (N, P) of the SOC and LAS groups immunostained by Ephrin B2, respectively. Ephrin B2 was expressed each group of the endothelial cell of the PA and PV. PA (Q, S) and PV (R, T) of the SOC and LAS groups immunostained by EphB4, respectively. EphB4 was not expressed in both groups. U-W, The wall thickness and vascular dimension of PV were increased in the LAS group. More distal veins with smaller PV dimension exhibited thicker PV wall, suggesting that distal PV veins are susceptible to LAS. X, PCNA-positive cells were more in the PVs of the LAS group. Original magnification ×40. *SOC,* Sham-operated control; *LAS,* left atrium stenosis; *PA,* pulmonary artery; *PV,* pulmonary vein; *EVG,* Elastica van Gieson; *SMA,* smooth muscle actin; *PCNA,* proliferating cell nuclear antigen. **$P < .01$, upper horizontal bar: third quartile, middle horizontal bar: middle quartile, lower horizontal bar: first quartile.

CONG
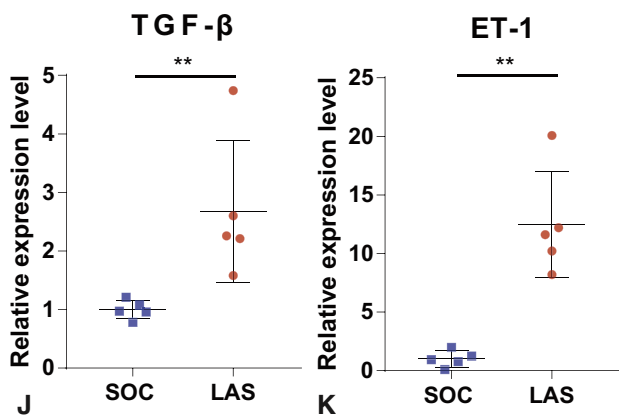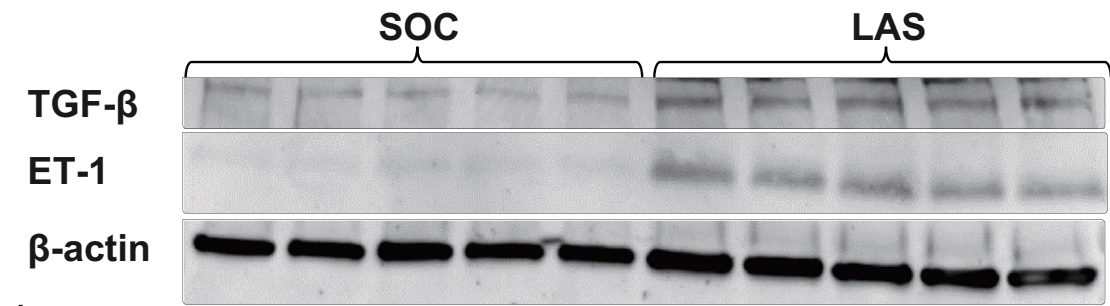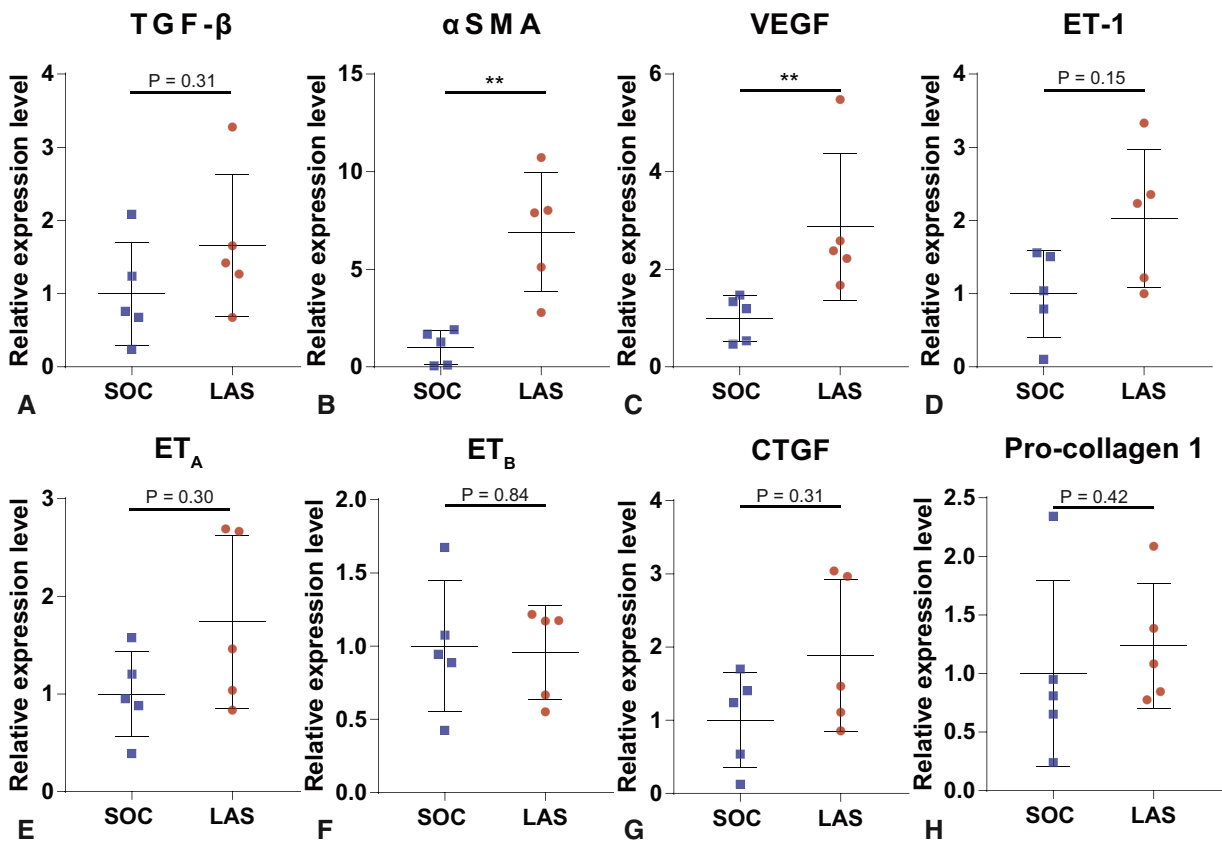
the systemic veins is caused by shear stress of pressure loads induced by an arteriovenous shunt. Ephrin B2 is specifically expressed in arterial endothelial cells and SMCs, whereas EphB4 is specifically expressed in veins during development. EphB4 is known to be downregulated in arterialized veins.[25] Considering that this mechanism is involved in arterialization of the PV in the present study, we examined immunostaining of Ephrin B2 and EphB4 in the lung of our LAS-induced PH-LHD model (Figure 4, M-T). However, EphB4 was not expressed in the SOC and LAS groups. We currently do not have a reasonable explanation for the discrepancy between our results and those of previous studies in systemic veins. Hall and colleagues[26] reported that Ephrin and Eph are mainly expressed during an embryonic period and involved in differentiation into the PA and vein, but their expressions are decreased after birth, suggesting that the involvement of Ephrin in arterialization of the PV is less likely.

We found that TGF-β and ET-1 expression levels were enhanced in the LAS lung on DNA microarray and Western blot analyses. Although real-time polymerase chain reaction analysis did not show the significant difference of them in the LAS and SOC groups, we think that it must be due to the small number of sample sizes. It has been reported that TGF-β and ET-1 are involved in PAH progression and enhanced in pulmonary arteries in response to shear stress, hypoxia, and thrombin.[27,28] In addition to these molecules, we also found that many genes that are changed in patients with PAH and animal models were similarly changed in the present DNA microarray analysis.

Clinical Implications

Although several drugs such as endothelin receptor antagonists, prostacyclin, and PDE-5 inhibitors are clinically used for patients with PAH, there is little consensus for treatment of PH-LHD because they have different pathophysiology compared with PAH. It should be noted that pediatric patients with cor triatriatum or who undergo supra-annular mitral valve replacement with LA reduction exhibit similar pathophysiology with the LAS model rat. As indicated earlier, the PV hydrostatic pressure is increased in most of patients with PH-LHD. In addition, some of these patients exhibit LV failure and low cardiac output. In the present study, ET-1 was increased in the PH-LHD model, suggesting that endothelin receptor antagonists may be effective for PH-LHD. Endothelin

receptor antagonists inhibit ventricular remodeling and improve exercise tolerance in an animal model of HF.[29] An endothelin receptor antagonist, tezosentan, was reported to increase cardiac output and reduce the pulmonary arterial wedge pressure and pulmonary and systemic vascular resistance in patients with acute HF.[30] However, the efficacy of long-term administration of endothelin receptor antagonists against chronic HF was not observed in the Research on Endothelin Antagonists in Chronic Heart Failure (REACH-1) study.[31] Perez-Villa and colleagues[32] recently reported that administration of an endothelin receptor antagonist, bosentan, for 4 months significantly reduced pulmonary vascular resistance in patients with PH who were indicated for cardiac transplantation.[32] PDE-5 inhibitors have been used mainly as a pulmonary vasodilator for PH-LHD.[4-6] However, the efficacy of PDE-5 inhibitors against PH-LHD is controversial, because Hoendermis and colleagues[7] reported that the PDE-5 inhibitor sildenafil did not improve pulmonary arterial pressure or clinical symptoms in patients with PH-LHD.[7] Therefore, the effect of these drugs in our LAS-induced PH-LHD rat model requires further study.

Study Limitations

One of the limitations in the present study is that we could not measure the LA and pulmonary capillary wedge pressure by catheterization because of bleeding. Therefore, we used the estimated LA pressure. Although the value of this estimated pressure was overestimated, we could not quantitatively investigate how LA pressure affects the pulmonary venous arterialization. Thus, the transpulmonary gradient is the important prognostic factor for patients with PH-LHD,[33] and detailed catheterization to estimate PV pressure is required in a future study. We also found that RV and LV end-diastolic pressures were increased in the LAS group, suggesting that elevated RV pressure may affect the diastolic LV function. This should be taken account for further investigation using this model.

It should be noted that we used the entire lung containing the artery, vein, bronchus, and alveolar epithelial cells for expression analyses. Further research is required to investigate a specific target that plays a critical role in development of PH-LHD, using pure PVs by cell sorting and immunohistochemical analyses.

The severity of PH was moderate, and only medial lesions were noted and no neointimal lesion was observed

FIGURE 6. mRNA and protein expression levels of the lung in the SOC and LAS groups. Real-time polymerase chain reaction analysis assessed the mRNA expression levels of (A) TGF-β1, (B) αSMA, (C) VEGF, (D) ET-1, (E) endothelin type A, (F) endothelin type B, (G) connective tissue growth factor, and (H) procollagen I. The expression levels of αSMA and VEGF were significantly increased in the LAS than in the SOC group. I, Western blot analyses revealed that the expression levels of (J) TGF-β1 and (K) ET-1 proteins were significantly increased in the LAS group. *SOC*, Sham-operated control; *LAS*, left atrium stenosis; *TGF-β*, transforming growth factor-β; *αSMA*, alpha smooth muscle actin; *VEGF*, vascular endothelial growth factor; *ET-1*, endothelin 1; *ET_A*, endothelin receptor type A; *ET_B*, endothelin receptor type B; *CTGF*, connective tissue growth factor. **$P < .01$, upper horizontal bar: third quartile, middle horizontal bar: middle quartile, lower horizontal bar: first quartile.

in the PV of the LAS rat. Because intimal lesions are usually thickened in patients with pulmonary veno-occlusive disease or PVS, we could not evaluate its mechanism by using this model.[34] Obviously, the obstruction in such diseases occur early during fetal development, and therefore, longer observation should be required to investigate the effect of the intimal lesions of the PV using this model.

CONCLUSIONS

We established a novel and feasible PH-LHD model in which venous arterialization was observed in rats. The LAS-induced PH-LHD model allows us to further investigate the mechanism of PH-LHD and treatments such as endothelin receptor antagonists.

Conflict of Interest Statement
Authors have nothing to disclose with regard to commercial support.

References

1. Guazzi M, Arena R. Pulmonary hypertension with left-sided heart disease. *Nat Rev Cardiol*. 2010;7:648-59.
2. Oudiz RJ. Pulmonary hypertension associated with left-sided heart disease. *Clin Chest Med*. 2007;28:233-41.
3. Nagy AI, Venkateshvaran A, Merkely B, Lund LH, Manouras A. Determinants and prognostic implications of the negative diastolic pulmonary pressure gradient in patients with pulmonary hypertension due to left heart disease. *Eur J Heart Fail*. 2017;19:88-97.
4. Lewis GD, Lachmann J, Camuso J, Lepore JJ, Shin J, Martinovic ME, et al. Sildenafil improves exercise hemodynamics and oxygen uptake in patients with systolic heart failure. *Circulation*. 2007;115:59-66.
5. Guazzi M, Samaja M, Arena R, Vicenzi M, Guazzi MD. Long-term use of sildenafil in the therapeutic management of heart failure. *J Am Coll Cardiol*. 2007;50:2136-44.
6. Guazzi M, Vicenzi M, Arena R, Guazzi MD. Pulmonary hypertension in heart failure with preserved ejection fraction: a target of phosphodiesterase-5 inhibition in a 1-year study. *Circulation*. 2011;124:164-74.
7. Hoendermis ES, Liu LC, Hummel YM, van der Meer P, de Boer RA, Berger RM, et al. Effects of sildenafil on invasive haemodynamics and exercise capacity in heart failure patients with preserved ejection fraction and pulmonary hypertension: a randomized controlled trial. *Eur Heart J*. 2015;36:2565-73.
8. Vonk Noordegraaf A, Groeneveldt JA, Bogaard HJ. Pulmonary hypertension. *Eur Respir Rev*. 2016;25:4-11.
9. Fujimoto Y, Urashima T, Shimura D, Ito R, Kawachi S, Kajimura I, et al. Low cardiac output leads hepatic fibrosis in right heart failure model rats. *PLoS One*. 2016;11:e0148666.
10. Ari H, Ari S, Karakus A, Camci S, Doganay K, Tutuncu A, et al. The impact of cardiac rhythm on the mitral valve area and gradient in patients with mitral stenosis. *Anatol J Cardiol*. May 24, 2017 [Epub ahead of print].
11. Wang Q, Guo YZ, Zhang YT, Xue JJ, Chen ZC, Cheng SY, et al. The effects and mechanism of atorvastatin on pulmonary hypertension due to left heart disease. *PLoS One*. 2016;11:e0157171.
12. Nishimura T, Vaszar LT, Faul JL, Zhao G, Berry GJ, Shi L, et al. Simvastatin rescues rats from fatal pulmonary hypertension by inducing apoptosis of neointimal smooth muscle cells. *Circulation*. 2003;108:1640-5.
13. Clark CB, Horn EM. Group 2 pulmonary hypertension: pulmonary venous hypertension: epidemiology and pathophysiology. *Cardiol Clin*. 2016;34:401-11.
14. Kato H, Fu YY, Zhu J, Wang L, Aafaqi S, Rahkonen O, et al. Pulmonary vein stenosis and the pathophysiology of "upstream" pulmonary veins. *J Thorac Cardiovasc Surg*. 2014;148:245-53.
15. Hunt JM, Bethea B, Liu X, Gandjeva A, Mammen PP, Stacher E, et al. Pulmonary veins in the normal lung and pulmonary hypertension due to left heart disease. *Am J Physiol Lung Cell Mol Physiol*. 2013;305:L725-36.
16. Yin J, Kukucka M, Hoffmann J, Sterner-Kock A, Burhenne J, Haefeli WE, et al. Sildenafil preserves lung endothelial function and prevents pulmonary vascular remodeling in a rat model of diastolic heart failure. *Circ Heart Fail*. 2011;4: 198-206.
17. Yang B, DeBenedictus C, Watt T, Farley S, Salita A, Hornsby W, et al. The impact of concomitant pulmonary hypertension on early and late outcomes following surgery for mitral stenosis. *J Thorac Cardiovasc Surg*. 2016;152: 394-400.e391.
18. Okada K, Tanaka Y, Bernstein M, Zhang W, Patterson GA, Botney MD. Pulmonary hemodynamics modify the rat pulmonary artery response to injury. A neointimal model of pulmonary hypertension. *Am J Pathol*. 1997;151:1019-25.
19. Taraseviciene-Stewart L, Kasahara Y, Alger L, Hirth P, McMahon G, Waltenberger J, et al. Inhibition of the VEGF receptor 2 combined with chronic hypoxia causes cell death-dependent pulmonary endothelial cell proliferation and severe pulmonary hypertension. *FASEB J*. 2001;15:427-38.
20. Taraseviciene-Stewart L, Nicolls MR, Kraskauskas D, Scerbavicius R, Burns N, Cool C, et al. Absence of T cells confers increased pulmonary arterial hypertension and vascular remodeling. *Am J Respir Crit Care Med*. 2007;175: 1280-9.
21. Ivy DD, McMurtry IF, Colvin K, Imamura M, Oka M, Lee DS, et al. Development of occlusive neointimal lesions in distal pulmonary arteries of endothelin B receptor-deficient rats: a new model of severe pulmonary arterial hypertension. *Circulation*. 2005;111:2988-96.
22. Merklinger SL, Wagner RA, Spiekerkoetter E, Hinek A, Knutsen RH, Kabir MG, et al. Increased fibulin-5 and elastin in S100A4/Mts1 mice with pulmonary hypertension. *Circ Res*. 2005;97:596-604.
23. Abe K, Toba M, Alzoubi A, Ito M, Fagan KA, Cool CD, et al. Formation of plexiform lesions in experimental severe pulmonary arterial hypertension. *Circulation*. 2010;121:2747-54.
24. Endo M, Yamaki S, Ohmi M, Tabayashi K. Pulmonary vascular changes induced by congenital obstruction of pulmonary venous return. *Ann Thorac Surg*. 2000; 69:193-7.
25. Kudo FA, Muto A, Maloney SP, Pimiento JM, Bergaya S, Fitzgerald TN, et al. Venous identity is lost but arterial identity is not gained during vein graft adaptation. *Arterioscler Thromb Vasc Biol*. 2007;27:1562-71.
26. Hall SM, Hislop AA, Haworth SG. Origin, differentiation, and maturation of human pulmonary veins. *Am J Respir Cell Mol Biol*. 2002;26:333-40.
27. Heath D. The rat is a poor animal model for the study of human pulmonary hypertension. *Cardioscience*. 1992;3:1-6.
28. Castanares C, Redondo-Horcajo M, Magan-Marchal N, ten Dijke P, Lamas S, Rodriguez-Pascual F. Signaling by ALK5 mediates TGF-beta-induced ET-1 expression in endothelial cells: a role for migration and proliferation. *J Cell Sci*. 2007;120:1256-66.
29. Miyauchi T, Fujimori A, Maeda S, Iemitsu M, Sakai S, Shikama H, et al. Chronic administration of an endothelin-A receptor antagonist improves exercise capacity in rats with myocardial infarction-induced congestive heart failure. *J Cardiovasc Pharmacol*. 2004;44(Suppl 1):S64-7.
30. Torre-Amione G, Young JB, Colucci WS, Lewis BS, Pratt C, Cotter G, et al. Hemodynamic and clinical effects of tezosentan, an intravenous dual endothelin receptor antagonist, in patients hospitalized for acute decompensated heart failure. *J Am Coll Cardiol*. 2003;42:140-7.
31. Packer M, McMurray J, Massie BM, Caspi A, Charlon V, Cohen-Solal A, et al. Clinical effects of endothelin receptor antagonism with bosentan in patients with severe chronic heart failure: results of a pilot study. *J Card Fail*. 2005;11: 12-20.
32. Perez-Villa F, Farrero M, Cardona M, Castel MA, Tatjer I, Penela D, et al. Bosentan in heart transplantation candidates with severe pulmonary hypertension: efficacy, safety and outcome after transplantation. *Clin Transplant*. 2013;27:25-31.
33. Yamabe S, Dohi Y, Fujisaki S, Higashi A, Kinoshita H, Sada Y, et al. Prognostic factors for survival in pulmonary hypertension due to left heart disease. *Circ J*. 2016;80:243-9.
34. Lo Rito M, Gazzaz T, Wilder TJ, Vanderlaan RD, Van Arsdell GS, Honjo O, et al. Pulmonary vein stenosis: severity and location predict survival after surgical repair. *J Thorac Cardiovasc Surg*. 2016;151:657-66. e651-652.

Key Words: pulmonary hypertension due to left heart disease, rat model, pulmonary vein
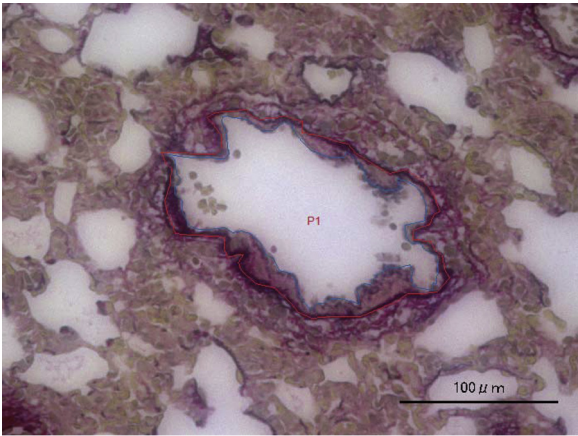
$$\text{Venous wall thickness} = \frac{\text{Red area} - \text{Blue area}}{\text{Red area}} \times 100$$

FIGURE E1. Measurement of pulmonary venous wall thickness. On Elastica van Gieson staining, the venous and venous luminal areas were measured using Image-Pro Premier 9.1 (Media Cybernetics, Rockville, Md). Original magnification: ×40.
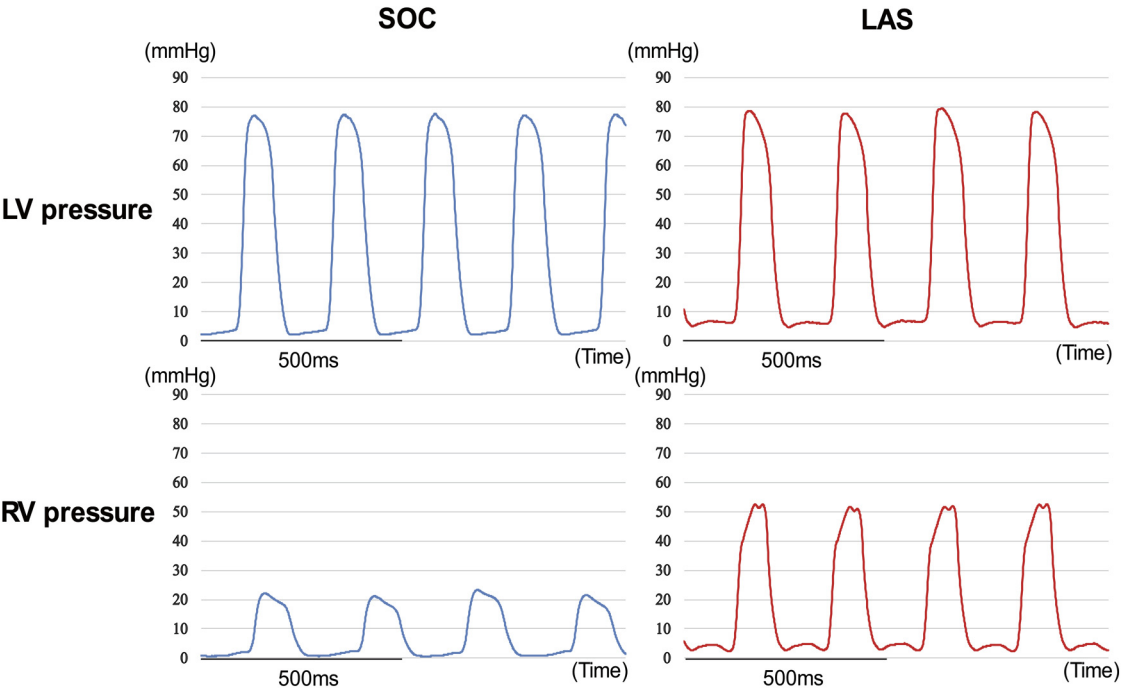
FIGURE E2. Pressure waveforms in the SOC and LAS groups. *SOC*, Sham-operated control; *LAS*, left atrium stenosis; *LV*, left ventricle; *RV*, right ventricle.

SOC   LAS
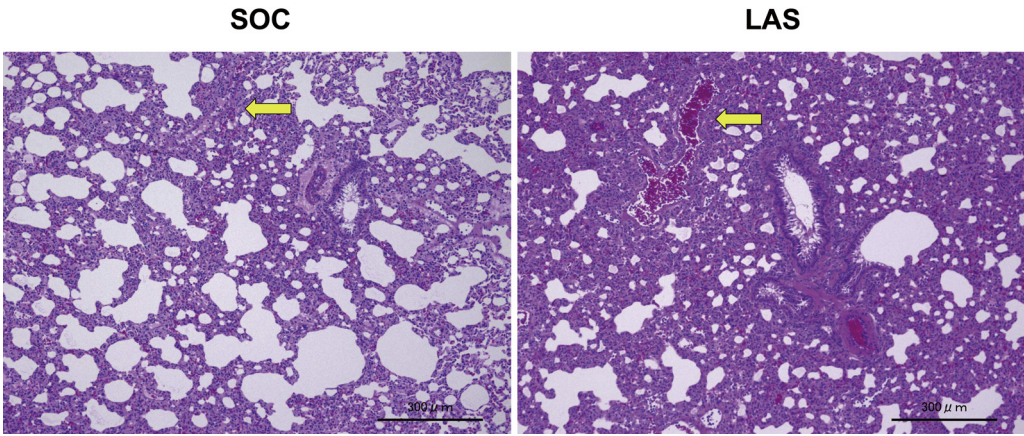
FIGURE E3. Hematoxylin–eosin stains of the lung in the SOC and LAS groups. On hematoxylin–eosin staining, pulmonary arteriovenous congestion and venous dilatation were noted in the LAS group. *Yellow arrow* indicates PV. *SOC*, Sham-operated control; *LAS*, left atrium stenosis. Original magnification: ×10.

CONG

Number of genes per concurrent annotations

46 genes

4 genes

4 genes

5 genes

5 genes

5 genes

5 genes

7 genes

9 genes

- Protein processing in endoplasmic reticulum
- Pathways in cancer
- TGF-beta signaling pathway
- RNA transport
- Phagosome
- Hepatitis C
- Insulin signaling pathway
- mRNA surveillance pathway
- Others

Protein processing in endoplasmic reticulum
Pathways in cancer
RNA transport
Hepatitis C
Phagosome
TGF-beta signaling pathway
mRNA surveillance pathway
Insulin signaling pathway
Chagas disease (American trypanosomiasis)
Pathways in cancer. Thyroid cancer
mTOR signaling pathway. Insulin signaling pathway
Glycerophospholipid metabolism
ErbB signaling pathway
Pathways in cancer. Prostate cancer
Complement and coagulation cascades
Toll-like receptor signaling pathway
Adherens junction
Protein digestion and absorption
Hepatitis C. TGF-beta signaling pathway. Oocyte meiosis. Chagas disease (American trypanos...
Acute myeloid leukemia
Tight junction. Wnt signaling pathway
Sphingolipid metabolism
Antigen processing and presentation

0   2   4   6   8   10

FIGURE E4. DNA microarray pathway analysis. Pathway analysis was performed by using genes expressed in the LAS group at a level of 4 times or more than those in the SOC group on microarray analysis. *TGF*, Transforming growth factor.

TABLE E1. List of primer sequences used for real-time polymerase chain reaction

Gene name	Forward primer	Reverse primer
18S	5′-AGCCTGAGAAACGGCTACC-3′	5′-TCCCAAGATCCAACTACGAG-3′
TGF-β1	5′-CTTTGTACAACAGCACCCGC-3′	5′-TAGATTGCGTTGTTGCGGTC-3′
αSMA	5′-TGTGCTGGACTCTGGAGATG-3′	5′-GATCACCTGCCCATCAGG-3′
VEGF	5′-CCGGACGGGCCTCTGAAACC-3′	5′-GGTGCAGCCTGGGACCACTTG-3′
ET-1	5′-TCTGGGTCAACACTCCCGA-3′	5′-AGGATCGCTTAGACCTAGAAGGG-3′
ET$_A$	5′-GGAATGGGAGCTTGCGG-3′	5′-TTTGCCACCTCTCGACGC-3′
ET$_B$	5′-CAAAGGAGGGAGGGTGGC-3′	5′-CAATTTTTCGTTGGCACGG-3′
CTGF	5′-CGGAGCGTGATCCCTGCGAC-3′	5′-GGTGCACCATCTTTGGCAGTGC-3′
Procollagen I	5′-GAGCGGAGAGTACTGGATCGA-3′	5′-CTGACCTGTCTCCATGTTGCA-3′

18S, 18S ribosomal RNA; *TGF-β1*, transforming growth factor-β1; *αSMA*, alpha smooth muscle actin; *VEGF*, vascular endothelial growth factor; *ET-1*, endothelin 1; *ET$_A$*, endothelin receptor type A; *ET$_B$*, endothelin receptor type B; *CTGF*, connective tissue growth factor.

CONG

TABLE E2. Genes expressed in the lung in LAS group at a level of 4 times or more than those in the sham-operated control group

Gene name	SOC	LAS
Hbg 1	32.15544	715.2045
Fibin	3.436082	67.8847
Cd300lg	1.954838	37.25043
RT1-O1	2.53117	44.84753
Acer2	18.46305	234.1399
Hs3st6	2.002269	23.9019
Ccng1	4.182419	46.85826
Prg4	3.099689	33.06003
Ighm	6.072891	60.74852
Ctnnb1	2.473024	22.78905
Ctss	2.784846	23.08603
Cd9	30.0338	245.8368
Slc3a2	4.203848	33.04954
Dpysl2	4.07708	31.87912
Chia	4.004959	31.20715
Asb3	2.436427	18.90138
Dpy19l1	2.085582	15.50285
Cndp2	7.626613	56.51087
Aqp5	2.614721	19.07379
Klkb1	11.92467	85.89598
Sptlc2	3.892384	27.8451
Sqrdl	10.99797	78.65548
Cdkn2b	1.665281	11.83019
Crebrf	1.763165	12.42472
Tpra1	1.582087	11.09518
Cdc14a	2.316994	16.16682
Emd	1.748951	12.00526
Dock9	4.377829	29.88537
Tspan9	4.533859	30.82217
Sec24d	1.676115	11.31154
Lyzl6	2.110511	14.08547
Ppp2ca	4.714699	31.4267
Dapk2	1.628922	10.82411
Flrt3	2.979898	19.69566
Pigf	3.038283	20.05364
Arl6ip1	3.606564	23.78064
Atp6v1b1	1.6654	10.97303
Abcb1b	40.09068	261.5699
Ube2f	3.229837	20.9403
Champ1	2.350092	15.12088
Sod2	1.738236	11.09988
Mri1	2.520336	15.96544
Fads3	7.156097	45.30926
Ppih	4.349044	27.35228

(Continued)

TABLE E2. Continued

Gene name	SOC	LAS
Mrps9	3.411153	21.44486
Ppp2cb	5.638615	35.39413
Ns5atp4	1.629399	10.21289
Lama3	4.63896	28.94726
Rbms1	23.77243	147.9272
Usp22	2.53117	15.70934
Enkur	4.240326	26.1023
Gbp5	1.643732	10.10306
Clpb	2.83506	17.39567
Arl6	2.83506	17.38518
Pi4kb	2.063676	12.56809
Prkag1	2.096416	12.67707
Hsp90aa1	74.45435	449.3569
Exo5	2.690579	16.2268
Herpud2	6.796487	40.97483
Ddx49	1.582206	9.514077
Kifap3	1.77388	10.66532
Mfas1	14.54017	87.18472
Pifo	1.954838	11.69653
Ccdc189	2.364425	14.05046
Capsl	4.280303	25.36277
Ostc	4.685675	27.70361
Mettl7a	8.615077	50.92659
Nedd9	2.617743	15.28102
Rpn2	13.49054	77.84222
Kank2	4.410689	25.39418
Nit2	3.725878	21.35608
C4bpa	5.518704	31.52604
Cyp2b1	57.371	327.0416
Fkbp5	75.82592	432.0099
Spata33	1.592921	9.069646
Lox	10.97281	62.43033
Tek	29.29144	164.9612
Rnf167	2.37514	13.2922
Tmem38b	4.374211	24.4511
Lyc2	9.680332	53.8908
Stx18	5.710974	31.65901
Arpc1a	4.569979	25.14861
Anxa7	6.298378	34.39662
Aldh2	39.82339	216.2054
Zmpste24	2.823868	15.30615
Plpp5	2.737653	14.82235
Hist1h2bk	6.724604	36.35284
Mrpl2	3.13569	16.90472

(Continued)

TABLE E2. Continued

Gene name	SOC	LAS
Cdadc1	2.650484	14.20183
Tmem30a	8.985164	48.13895
Chit1	3.932122	20.93161
Usf2	1.987817	10.57189
Ano10	4.240445	22.51953
Mrpl49	3.566826	18.8046
Triap1	7.64852	40.21016
Tmem248	3.541778	18.56955
Akr1b8	10.70865	56.0489
Timp2	44.6147	232.9254
Zfp148	6.07313	31.7023
RT1-CE2	16.45315	85.86081
Mterf4	2.303138	12.01036
Dnajc19	2.16144	11.26361
Inmt	55.33159	287.9427
Pkd2	2.303138	11.94904
Zfp709	1.726925	8.953124
Pgm2	9.962554	51.35747
Fkbp4	11.00916	56.65032
Ssr3	1.748832	8.994086
Hexb	6.217968	31.97745
Gpn3	2.676127	13.73023
Dhx32	2.194181	11.255
Sgms1	2.002389	10.24541
Cdc73	3.591993	18.37151
Rnf139	6.10925	31.17786
Zfp68	3.001924	15.28636
Rnpc3	2.940518	14.96939
Snrpa1	3.34927	16.96707
Lmcd1	18.71287	94.79536
Scimp	3.110404	15.7516
Papss1	9.15505	46.34667
Xpnpep2	5.026043	25.36065
Map2k4	1.581968	7.981438
Pcdhgb7	2.147108	10.82513
Vamp4	2.233681	11.25704
G3bp2	1.85755	9.347695
Ifit1bl	2.146988	10.79013
Ins2	15.12781	75.69355
Pus3	2.41126	12.05961
Wdr61	3.817003	19.05046
Rassf7	2.00215	9.983477
Etv1	6.724962	33.4896
F11	2.339377	11.64439

(Continued)

TABLE E2. Continued

Gene name	SOC	LAS
Tlr3	8.010437	39.73582
Klk6	5.048546	25.00508
Papola	4.78344	23.67399
Rtn4	16.40245	81.1261
Serinc1	46.77354	230.9345
Zbtb16	38.40681	189.5025
Gpx3	8.445191	41.64545
Pxdc1	8.121938	39.97312
Pcbd1	1.857192	9.138638
Entpd4	1.919195	9.440556
Efl1	3.135452	15.40583
Tpst1	2.943659	14.44141
Sqstm1	3.084999	15.02068
Adam9	7.456012	36.26235
Oas1a	2.748368	13.36181
Ly6e	14.16332	68.63725
Ddx28	2.777033	13.4055
Fxyd6	1.59316	7.685927
Mrc1	20.71568	99.67222
Pcgf5	2.929326	14.09143
Arhgef28	15.52561	74.47576
Sars	5.953458	28.55514
Ryk	8.083154	38.70865
Esm1	97.64001	466.2564
Comt	4.095488	19.50093
Fam189a2	11.88974	56.57089
Wdr18	2.868039	13.60758
Chpt1	1.940744	9.204326
Spg21	10.56358	50.08448
Ctdspl	20.31319	96.14566
U2af1l4	9.096904	42.83186
Ephx2	3.335176	15.65177
Rn50_X_0616.3	3.027687	14.20212
Zdhhc20	1.951697	9.147247
Raly	3.581158	16.78383
Cldn18	15.97446	74.69069
Ssr2	18.62944	87.05722
Zmat5	4.026269	18.80085
Fam63a	3.664471	17.0618
Rad23a	10.15109	47.20774
Tacstd2	6.14537	28.4553
Arcn1	1.592921	7.360673
Ttc30a1	2.0892	9.648756
Trem2	6.902422	31.8384

(Continued)

CONG

TABLE E2. Continued

Gene name	SOC	LAS
Wwc3	2.364425	10.89967
Pecr	22.82252	104.545
Nudcd2	2.472666	11.29947
Krt19	84.13438	383.6586
Arhgap29	1.73764	7.92232
Rragc	4.171704	18.9871
Pgp	3.291363	14.96923
Ubr3	3.121477	14.16597
Tmco3	2.027555	9.200409
ST7	3.737189	16.91749
Rpp30	3.411153	15.43402
Pdha1l1	2.461951	11.13097
Noxo1	2.158538	9.75916
Ppp2r3c	2.361165	10.65545
Mgea5	2.111107	9.5244
Hes1	2.773177	12.50999
Ift52	5.315601	23.88656
Cfap43	1.774357	7.933826
Ngly1	9.060664	40.42579
Ankmy2	2.378638	10.59861
Gpd2	7.228338	32.17157
Unc5b	4.41057	19.6121
Ier5	4.638602	20.57489
Fam192a	2.42595	10.75569
Clec14a	31.50409	139.6666
Gsr	1.810119	8.024728
Atp5a1	60.2096	266.5212
Xbp1	2.204896	9.753203
Kdm1a	1.89379	8.359324
Ctsc	1.835524	8.101145
Derl2	8.915945	39.345
Vps52	5.54411	24.38415
Clca1	3.349628	14.73182
Zfp868	1.893313	8.316485
Gtf2e2	4.928517	21.62912
Fbxo18	5.250696	23.02222
Ptdss1	3.66471	16.03606
Smad4	3.50868	15.26935
Prss12	5.555063	24.09602
Zfp472	2.255707	9.774419
Kmt5b	3.255123	14.10004
Exd2	1.665519	7.213468
Lrrc51	3.422107	14.81264
Hipk2	1.773641	7.666751

(Continued)

TABLE E2. Continued

Gene name	SOC	LAS
Slc35b3	4.592005	19.84528
Fgg	24.25438	104.8088
Plrg1	11.45451	49.48493
Capn2	36.80311	158.9424
Efhc1	3.316649	14.3217
Prdm6	2.628577	11.3339
Zfp717	7.409296	31.94726
Usp25	2.676008	11.53774
Fst	8.035485	34.54656
Slc24a4	2.773296	11.92305
Pparg	3.676021	15.78763
Tmem208	13.06626	56.07676
Mmadhc	5.833906	25.0163
Baiap2	6.120084	26.22344
Rps4y2	9.683831	41.38919
Slc39a2	6.963947	29.67513
Nsf	2.15818	9.1918
Mapk1	5.265506	22.41492
Ddx18	1.59304	6.779361
Klhl24	17.05357	72.37992
Clptm1	2.700937	11.46234
Rnpep	5.001234	21.20284
Csde1	29.79191	126.0203
Rbfa	2.436784	10.30632
Eif4e	2.437023	10.28947
Clic3	52.51696	221.6995
Lztfl1	2.976638	12.54875
Dync1i2	11.98353	50.47722
Rspo1	1.860691	7.826563
Sec13	11.15086	46.89926
Sdhb	33.60212	141.3081
Sec24c	3.280409	13.79473
Mfsd1	2.520336	10.59572
Emc4	31.03405	130.1997
Nek6	3.02721	12.69698
Cryl1	1.955196	8.193312
Hebp1	19.65414	82.32838
Galnt14	2.759202	11.55691
Nup37	2.37502	9.944717
Sypl1	6.736034	28.14718
Rnf122	1.991793	8.314445
Vps37a	3.121715	13.03084
Jtb	7.083499	29.55252
Nckap1	6.988875	29.14339

(Continued)

TABLE E2. Continued

Gene name	SOC	LAS
Tceb1	2.146988	8.943657
Ppib	42.7424	177.6466
Oraov1	2.411498	10.0195
Cd83	1.785071	7.404369
Mccc2	13.54028	56.11475
Apoa1bp	11.86796	49.18253
Ptbp1	2.509263	10.3656
Armcx1	4.084534	16.86927
Thap11	8.419666	34.72351
Tnpo1	2.592934	10.6672
Esd	15.34418	63.11727
Atp11b	2.531051	10.40481
Hacd3	3.943076	16.19542
Rnf13	3.399961	13.95907
Noa1	2.581861	10.59078
Pdxdc1	1.581848	6.486459

(Continued)

TABLE E2. Continued

Gene name	SOC	LAS
Pcmtd2	7.637924	31.31568
Bst1	5.797189	23.72254
Fahd1	3.555634	14.5443
Ube2v2	10.21949	41.75181
Lpin2	2.712605	11.06818
Kcne3	9.502634	38.76708
Klc1	6.601672	26.87623
Acat1	6.71051	27.31352
Tmem242	3.519394	14.30587
Rpa1	2.98783	12.06471
Sdf2l1	17.31808	69.92942
Shmt1	6.03689	24.36453
Fbxo8	9.770762	39.37801
Eif4ebp1	7.253028	29.17872
Atxn10	13.33415	53.40831

SOC, Sham-operated control; *LAS*, left atrium stenosis.

CONG